

Structure and Properties of Titanium-Including Complex, Tris(tetramethyltetrathiafulvalene) Di- μ -fluoro-bis[tetrafluorotitanate- (IV)], (TMTTF)₃Ti₂F₁₀

Hiroki Akutsu, Katsunari Ozeki, Takayuki Ozaki, Kiyokazu Nozawa,[†] Minoru Kinoshita,[†]

Kozo Kozawa, and Tokiko Uchida*

Department of Industrial and Engineering Chemistry, Faculty of Science and Technology, Science University of Tokyo,
2641, Yamazaki, Noda, Chiba 278

[†]The Institute for Solid State Physics, The University of Tokyo, Roppongi, Minato-ku, Tokyo 106

(Received January 8, 1996)

A novel molecular complex of tetramethyltetrathiafulvalene (TMTTF) was prepared by the treatment with TiF₄. The X-ray analysis reveals the existence of a trimer of TMTTF's and a Ti₂F₁₀²⁻ anion in a triclinic unit cell of the dimension; $a = 10.934(3)$, $b = 12.798(2)$, $c = 8.000(1)$ Å, $\alpha = 103.86(1)$, $\beta = 107.08(2)$, $\gamma = 75.02(2)^\circ$. All the molecular planes of TMTTF are nearly parallel. The trimers stack parallel to the a axis, and the intertrimer interaction is estimated to be weak. A semiconductive behavior with a relatively large Seebeck coefficient was observed ($\rho = 3 \times 10^2$ Ω cm, $E_a = 0.26$ eV, and $S = -0.41$ mV K⁻¹ along the a axis). Weak electron spin resonance (ESR) absorption was observed to be characteristic of low-dimensional diffusive spin systems.

Studies of the solid-state properties of organic conductors, which include transition metals having localized magnetic moments on their d orbitals, have been actively developed in the recent decade.¹⁻⁴ During the studies of copper N,N' -dicyano- p -benzoquinonediimine [(DCNQI)₂Cu] and their homologue systems, the interactions between d orbitals of transition metals and conduction bands have been discussed.⁵ However, uses of transition metals, having no localized magnetic moments on their d orbitals, are seldom found in this field.

In this paper, we would like to report the crystal and electronic structure of a novel ionic complex compound, tris(tetramethyltetrathiafulvalene) di- μ -fluoro-bis[tetrafluorotitanate(IV)], (TMTTF)₃Ti₂F₁₀.

Experimental

Complex Formation. Acetonitrile solutions of tetramethyltetrathiafulvalene (TMTTF) and TiF₄ (Aldrich) (each concentration was 1×10^{-3} mol dm⁻³) were mixed at about 1 : 1 mol ratio. By slow evaporation of the solvent in a dry atmosphere, black columnar or plate-like crystals were obtained. Their typical size was $0.5 \times 0.3 \times 0.1$ mm³.

X-Ray Data Collection. A plate-like crystal about $0.4 \times 0.3 \times 0.1$ mm³ was mounted on a Rigaku AFC-5 four-circle diffractometer with graphite-monochromatized Mo $K\alpha$ radiation ($\lambda = 0.71073$ Å). Lattice parameters were determined with 20 ($28^\circ \leq 2\theta \leq 32^\circ$) reflections. Diffraction data were collected in $\theta/2\theta$ mode with scan width $(1 + 0.35 \tan \theta)^\circ$ in θ , scan rate at 4° min⁻¹ in θ , and scan range $2\theta_{\max} \leq 60^\circ$. Three standard reflections: (0 -8 3, -2 -1 6, -3 -6 5) were monitored at every 100 measurements and intensity variations were within 2% in F . Of the 6340 reflections measured,

3919 reflections were observed with $|F_o| > 3\sigma(|F_o|)$.

Structure was solved by the direct method, and refined by block-diagonal least-squares refinement. The quantity minimized was $\sum w(|F_o| - |F_c|)^2$, with $w = 1/\sigma^2(|F_o|)$. Refined parameters are atomic coordinates for all the atoms and anisotropic temperature factors for non-hydrogen atoms. The isotropic temperature factor for hydrogen atoms was fixed at $B_{\text{iso}} = 4.0$ Å². Residuals were converged to $R = 0.061$ and $R_w = 0.028$ for 3919 reflections. Scattering factors and anomalous dispersion factors for Ti and S were taken from International Tables for X-ray Crystallography.⁶ Calculations were carried out on a Panafacom U-1200II computer with the Rigaku RASA-5P program package and on a HITAC M-880 at the Computer Centre of the University of Tokyo with the UNICS program system.⁷

Resistivity and Seebeck Coefficient. The electrical resistivity (ρ) along the three axes and Seebeck coefficient (S) along the a axis (growing axis) were observed over the range from 220 K to room temperature. Seebeck coefficients along the b and c axes were observed only at room temperature. Resistivity was measured by a four-probe d.c. technique along the a axis, and by a two-probe technique for the other two directions. Carbon paint was applied as the contacts between electrodes ($25 \mu\text{m}$ ϕ gold wire) and the crystal specimen. One end of the specimen was attached to a copper heat sink, and the other end of the specimen was attached to the other heat sink. During the Seebeck coefficient observations, the temperature difference between the two heat sinks was controlled to 0.5° or 1.0° . The observed Seebeck coefficient value was an average of the values from these two observations.

Pressure Dependence of Resistivity. A clamp type pressure cell was used with an oil (Daphne #7373) as a pressure medium. The temperature dependence of electrical resistivity was measured with the same specimens under three different pressures: 3, 6 and 9 kbar.

Electron Spin Resonance (ESR). Angular dependence of the resonance field was observed about a single crystal ($0.5 \times 0.25 \times 0.15$ mm³) with a JEOL JES-FE1XG X-band (9.1 GHz) ESR spectrometer and a two-circle goniometer. The rotation axes of the crystal, **X**, **Y**, and **Z**, were defined as follows; **X**//**a**, **Y**//**b**^{*}, and **Z** was perpendicular to both **X** and **Y**, where the external magnetic field was parallel to the **b**^{*}**c**^{*} plane, **ac** plane, and **ab**^{*} plane, respectively. The *g* value was estimated by use of the standard material Li·TCNQ (*g*=2.0026). The line width was taken as the peak-to-peak width, ΔH_{pp} . The spin density was assumed by comparing the integrated value with that of violanthrone.

Results and Discussion

Crystal Structure. Crystal data: (C₁₀H₁₂S₄)₃Ti₂F₁₀, F. W. = 1067.15, triclinic, space group $P\bar{1}$, *a* = 10.934(3), *b* = 12.798(2), *c* = 8.000(1) Å, α = 103.86(1), β = 107.08(2), γ = 75.02(2)°, *V* = 1017.4(4) Å³, *Z* = 1, *D*₀ = 1.73, *D*_x = 1.74 Mg m⁻³, $\mu(\text{Mo } K\alpha)$ = 1.07 mm⁻¹. Since there are three TMTTF molecules and a Ti₂F₁₀ anion in a centrosymmetric unit cell, an asymmetric unit of the cell includes one and a half TMTTF molecules and a half of one Ti₂F₁₀ anion. Figure 1 shows the crystal structure and Table 1 shows atomic parameters.⁸⁾ The atom numbering of TMTTF moieties is described in Fig. 2 along with the geometric parameters. All the TMTTF molecules are parallel within the estimated standard deviations (esd's), making a trimerized structure. Each trimer locates on a crystallographic inversion center, and the trimers stack along the *a* axis. The angle between the normal of the molecular plane of TMTTF (hereafter, plane-normal) and the *a* axis is 13.3°. The interplanar distance in a trimer of 3.46 Å is a value comparable with those observed in many dimerized (TMTTF)₂X (X = Br, BF₄, SCN, I etc.),⁹⁾ which possess high electrical conductivity along the stacking direction.¹⁰⁾ The molecular overlapping manner in a trimer, illustrated in Fig. 3(a), also suggests the presence of fairly strong interaction inside a trimer. On the other hand, the interplanar distance of 3.67 Å, and poor molecular overlap between the two neighboring trimers, as shown in Fig. 3(b), imply that the intertrimer interaction is much weaker than the intratrimer one. There are no specially short intermolecular

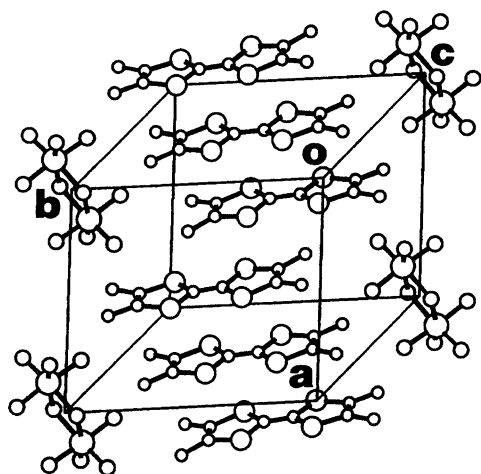


Fig. 1. Crystal structure of (TMTTF)₃Ti₂F₁₀.

Table 1. Fractional Coordinates and Equivalent Isotropic Thermal Parameters for Non-Hydrogen Atoms, with esd's in Parentheses

Atom	<i>x</i>	<i>y</i>	<i>z</i>	<i>B</i> _{eq} ^{a)} /Å ²
Ti	-0.15591(7)	0.05502(6)	-0.0399(1)	2.42(2)
F(1)	-0.2339(2)	0.1898(2)	0.0436(3)	4.8(1)
F(2)	-0.2927(2)	-0.0041(2)	-0.1748(3)	4.69(9)
F(3)	-0.1618(2)	0.0048(2)	0.1517(3)	3.60(8)
F(4)	-0.1372(2)	0.0995(2)	-0.2287(3)	3.69(8)
F(5)	0.0242(2)	0.0838(2)	0.0924(3)	2.73(7)
S(11)	0.66499(9)	-0.21351(7)	0.5100(1)	2.46(3)
S(12)	0.62079(9)	-0.34226(7)	0.1509(1)	2.71(3)
S(13)	0.69287(9)	-0.43062(7)	0.6707(1)	2.61(3)
S(14)	0.66005(9)	-0.56254(7)	0.3134(1)	2.57(3)
S(21)	-0.00043(9)	0.67371(7)	0.5999(1)	2.33(3)
S(22)	-0.03675(9)	0.54724(7)	0.2434(1)	2.35(3)
C(10)	0.6252(3)	-0.0203(3)	0.3782(5)	3.0(1)
C(11)	0.5753(4)	-0.1580(3)	0.0008(5)	3.5(1)
C(12)	0.6308(3)	-0.1427(3)	0.3343(5)	2.2(1)
C(13)	0.6109(3)	-0.2020(3)	0.1711(5)	2.5(1)
C(14)	0.6524(3)	-0.3410(3)	0.3776(5)	2.3(1)
C(15)	0.6679(3)	-0.4328(3)	0.4445(5)	2.2(1)
C(16)	0.6911(3)	-0.5694(3)	0.6505(5)	2.4(1)
C(17)	0.6766(3)	-0.6298(3)	0.4879(5)	2.3(1)
C(18)	0.7056(4)	-0.6077(3)	0.8213(5)	3.5(1)
C(19)	0.6701(4)	-0.7500(3)	0.4353(5)	3.1(1)
C(20)	-0.0261(4)	0.8664(3)	0.4850(5)	2.8(1)
C(21)	-0.0681(4)	0.7286(3)	0.0934(5)	2.9(1)
C(22)	-0.0244(3)	0.7463(3)	0.4301(4)	2.1(1)
C(23)	-0.0411(3)	0.6867(3)	0.2648(5)	2.1(1)
C(24)	-0.0096(3)	0.5473(3)	0.4669(5)	2.2(1)

$$a) B_{eq} = (4/3) \sum_i \sum_j B_{ij} a_i \cdot a_j.$$

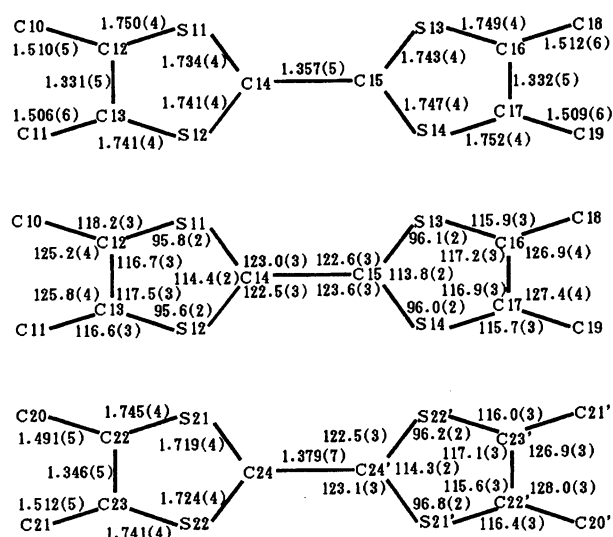


Fig. 2. Bond lengths (Å) and bond angles (°) of TMTTF molecules.

atomic distances between the neighboring donor stacks.

A Ti₂F₁₀ anion locates on a crystallographic inversion center. Each titanium atom is octahedrally coordinated by six fluorine atoms, two of which [F(5) and F(5')] are used for bridging the two titanium atoms. Geometric parameters

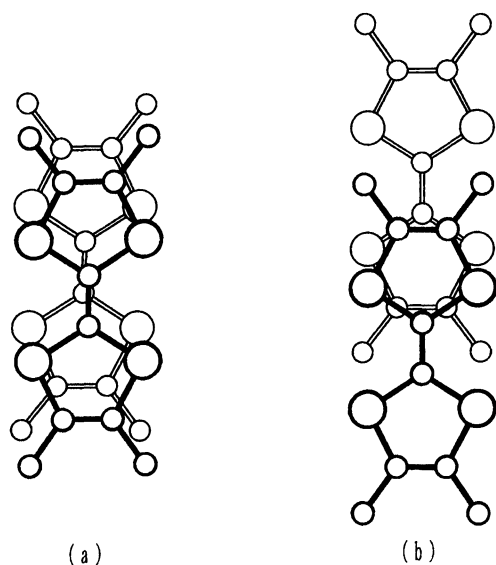


Fig. 3. Molecular overlap of TMTTF's. (a) Intratrimer; and (b) intertrimer.

of a Ti_2F_{10} are shown in Table 2. Bond distances of Ti-F's are almost in the range of those observed in tris(tetramethyltetraselenafulvalene)- μ -(oxalato- $O, O''': O', O''$)-bis[tetrafluorotitanate] in which the valence of Ti has been estimated as Ti(IV).¹¹⁾ Assuming the oxidation number also as Ti(IV) in this complex, Ti_2F_{10} anion carries a charge of -2 , and a TMTTF trimer carries an average charge of $+2$; namely, the average charge of a TMTTF is estimated as $+2/3$.

The intermolecular distances between the methyl carbon atoms of TMTTF's and their neighboring F atoms of Ti_2F_{10} 's are in the range of 3.250(4)–3.366(4) Å, which is slightly shorter than the generally accepted value of van der Waals contacts, 3.35–3.47 Å.

ESR. Observed angular dependences of g values and line widths around the **X**, **Y** and **Z** axes, are shown in Fig. 4. Around the **X** axis (the trimer-stacking direction) rotation, angular dependences of both g value and ΔH_{pp} vary almost sinusoidally with period of 180° . On the other hand, the angular dependence curves of ΔH_{pp} , both around **Y** and **Z** rotations, have two maxima (magnetic field at about 10° and 105° angles from the **X** axis) and two minima (magnetic field at about 65° and 140° angles from the **X** axis), though the

g value dependences are also sinusoidal with 180° period for both of them. From the observed angular dependences of the g values, their main values were estimated as follows: $g_1 = 2.0138$, $g_2 = 2.0083$, $g_3 = 2.0018$. These g values are comparative with other TMTTF complexes.¹⁰⁾ The direction of g_3 agrees with the plane-normal direction, and those of the g_1 and g_2 are in the donor plane. At the first maximum of ΔH_{pp} in Figs. 4(b) and (c), the direction of external magnetic field approximately agrees with the g_3 direction. In each of the same Figures, the difference between the first maximum and the first minimum is observed to be about 55° . This observation can be explained by the spin diffusion in a low-dimensional system.¹²⁾ Taking the plane-normal direction as the unique axis, the angular dependence of the absorption line width, ΔH , is expressed by Heisenberg model,

$$\Delta H = A(3 \cos^2 \Theta - 1)^n + B, \quad (1)$$

where $n=4/3$ for one-dimensional, and $n=2$ for two-dimensional exchange interaction. Θ is the angle between the external magnetic field and the unique axis. A and B are constants depending on the experimental conditions. In our case, ΔH is replaced to ΔH_{pp} . Whether the exchange interaction is one- or two-dimensional, ΔH_{pp} shows a minimum at the magic angle ($\Theta=54.7^\circ$), at almost the same value as our observation. So, if our observation can be elucidated by this model, spin interactions in the present complex are limited either in the plane-normal direction (one-dimensional) or in the plane in accord with the donor plane (two-dimensional). At the position where the sharpest ESR absorption peak was observed, the spin density was roughly estimated as low as $1/500$ for a TMTTF trimer about all the directions observed. Since the ESR signal was too weak to observe its temperature dependence, we could not determine whether the origin of the weak signal is fundamental to the present complex or not (paramagnetic impurity). In this connection, Scott et al. observed very weak but essential spin density in $(\text{TMTSF})_2\text{PF}_6$, which they elucidated by resonance between the ground state and antiferromagnetic state.¹³⁾ Assuming that the observed weak signal is essential to the present complex, we can suggest that there exist local electrons, and that they interact together in the low-dimensional long range order. However, we can not determine the dimensionality (one- or two-) in this system from the present experiments.

Electrical Resistivity. Under ambient pressure, a semi-conducting behavior was observed along the three axes examined. Table 3 describes the observed value of resistivity at room temperature and its activation energy (E_a). There is no evidence for anisotropic conduction, and the resistivity data tend to be sample-dependent for the b and c directions. On applying pressures, the observed resistivity and its activation energy along the a axis decreased monotonously, as shown in Fig. 5. Their decrease ratios were in the range of values for usual organic conductors.

Thermoelectric Power. Table 3 shows the Seebeck coefficients observed along the a , b , and c axis, respectively. They have two characteristic features: (1) the sign is neg-

Table 2. Bond Distances and Angles of Ti_2F_{10}

Bond distances/Å			
Ti-F(1)	1.781(3)	Ti-F(4)	1.817(2)
Ti-F(2)	1.794(3)	Ti-F(5)	2.024(2)
Ti-F(3)	1.822(2)		
Bond angles/ $^\circ$			
Ti-F(5)-Ti'	107.8(1)	F(1)-Ti-F(2)	101.9(1)
F(1)-Ti-F(3)	90.9(1)	F(1)-Ti-F(4)	92.2(1)
F(1)-Ti-F(5)	92.5(1)	F(2)-Ti-F(3)	90.8(1)
F(2)-Ti-F(4)	91.6(1)	F(2)-Ti-F(5)	165.6(1)
F(3)-Ti-F(4)	175.6(1)	F(3)-Ti-F(5)	88.7(1)
F(4)-Ti-F(5)	88.1(1)	F(5)-Ti-F(5')	72.16(8)

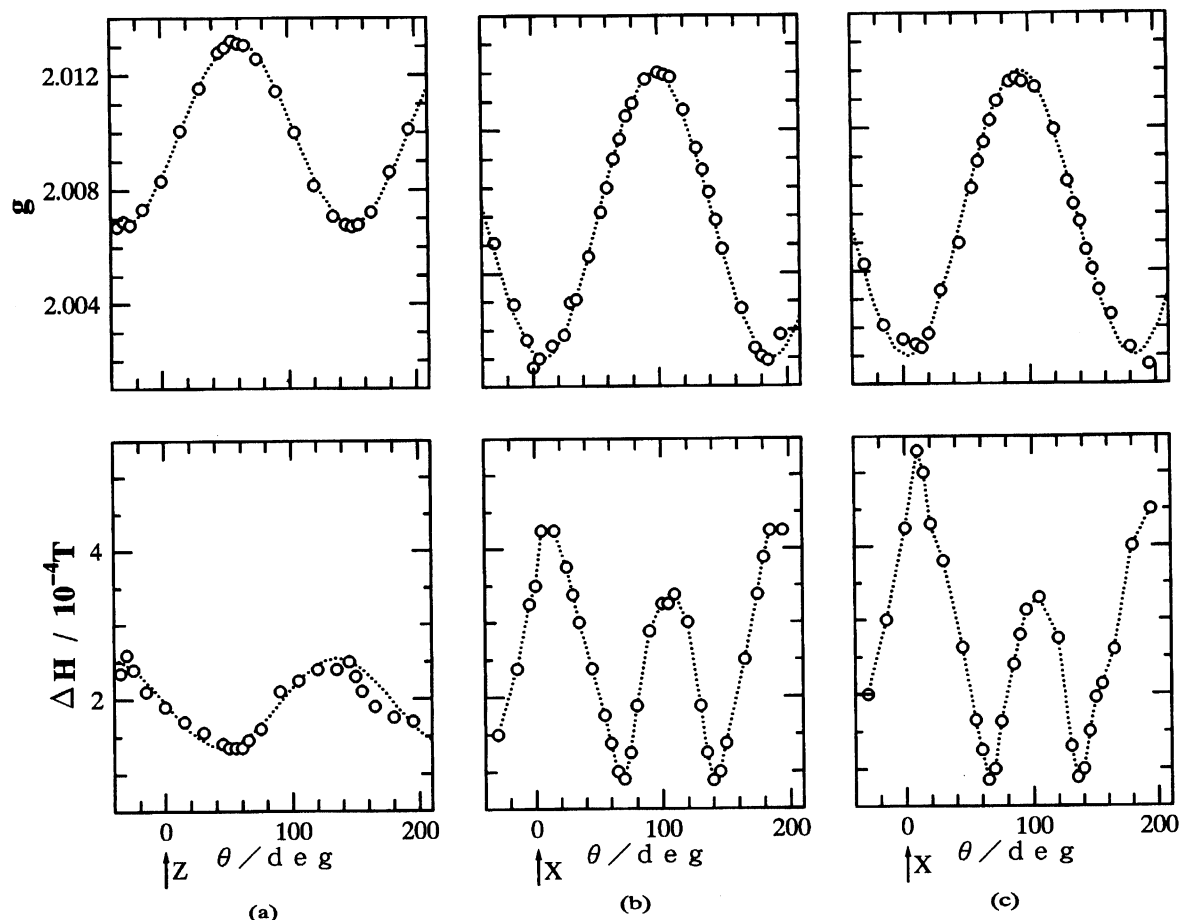


Fig. 4. Angular dependences of g value and absorption band width, ΔH_{pp} of ESR. Magnetic field were rotated in the b^*c^* plane (a), ac plane (b) and ab^* plane (c), respectively.

Table 3. Electrical Properties of (TMTTF)₃Ti₂F₁₀

Direction	Seebeck coef. $S/\mu\text{VK}^{-1}$	Resistivity	
		$\rho/\Omega\text{ cm}$	E_a/eV
a	-4.1×10^2	3×10^2	0.26
b	-2.0×10^2	10^2	0.2
c	-1.7×10^2	10^2	0.2

ative and the absolute values of them are larger, by about one or two orders of magnitude than the values of usual organic conductors or semiconductors,^{1,2,14)} and (2) the value along the a axis is more than two times as large as those along the other two axes. For these observations, there were no sample-dependences as mentioned in the resistivity section. As shown in Fig. 6, a temperature dependence of S observed along the a axis exhibits that S varies linearly with the reciprocal of temperature.¹⁵⁾

Electronic Structure. The observed results, cited above, can be summarized as follows.

(1) The crystal consists of TMTTF trimers and Ti₂F₁₀ anions. The stacking direction of the TMTTF trimers is parallel to the a axis, and the “intertrimer” interaction is weaker than the “intratrimer” one.

(2) Analysis of ESR measurements by “low-dimensional spin

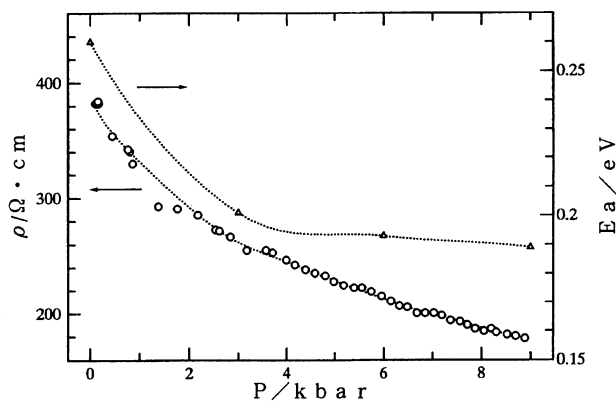


Fig. 5. Pressure dependences of electrical resistivity (open circle) and activation energy (triangle).

diffusion” model, suggests the existence of a low-dimensional exchange interaction between the TMTTF trimers, though the ESR signal was weak.

(3) Electrical resistivity exhibits isotropic and semiconductive behavior.

(4) Seebeck coefficients possess negative signs and their large absolute values suggest the electron conduction. The S value along the a axis is more than two times as large as those along the other two axes.

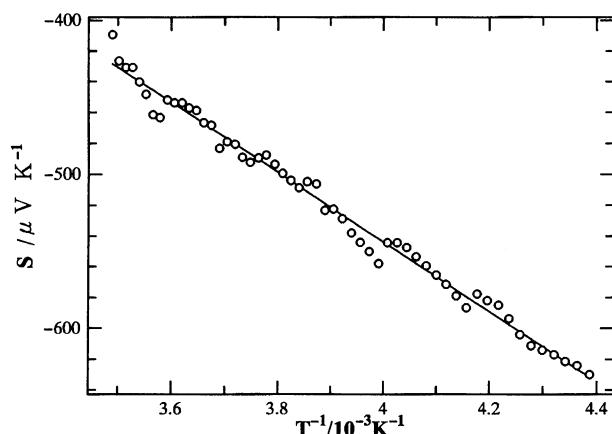


Fig. 6. Temperature dependence of the Seebeck coefficient observed along the *a* axis.

The isotropic behavior of electric resistivity and anisotropy of Seebeck coefficient suggest the possibility that the two-dimensional interaction, perpendicular to the stacking direction, is slightly larger than the one-dimensional interaction along the stacking direction. If there is some two-dimensional exchange interaction between the TMTTF trimers, we can not deny the possibility of the Ti_2F_{10} anions to participate in it by structural considerations. In such interactions, the empty *d* orbitals of Ti(IV) will play some part.

The authors would like to thank Professor Hiroyuki Anzai of Himeji Institute of Technology for providing purified TMTTF.

References

- 1) M. Inoue, M. B. Inoue, C. Cruz-Vazquez, S. Roberts, and Q. Fernando, *Synth. Met.*, **19**, 641 (1987).
- 2) M. B. Inoue, C. Cruz-Vazquez, M. Inoue, G. J. Pyrká, K. W. Nebesny, and Q. Fernando, *Synth. Met.*, **22**, 231 (1988).
- 3) P. Batail, L. Ouahab, J. B. Torrance, M. L. Pylman, and S. S. P. Parkin, *Solid State Commun.*, **55**, 597 (1985).
- 4) T. Sugano, H. Takenouchi, D. Shiomi, and M. Kinoshita, *Synth. Met.*, **42**, 2217 (1991).
- 5) S. Tomić, D. Jérôme, A. Aumüller, P. Erk, S. Hünig, and J. U. von Schütz, *J. Phys. C: Solid State Phys.*, **21**, L203 (1988).
- 6) "International Tables for X-Ray Crystallography," Kynoch Press, Birmingham, England (1974), Vol. IV.
- 7) T. Sakurai, "Universal Crystallographic Computation Program System," The Crystallographic Society of Japan, Tokyo (1967).
- 8) The $F_o - F_c$ table, the anisotropic temperature parameters, and hydrogen atom parameters are deposited as Document No. 69039 at the Office of the Editor of Bull. Chem. Soc. Jpn.
- 9) J. L. Galigné, B. Liautard, S. Peytavin, G. Brun, J. M. Fabre, E. Torrelles, and L. Giral, *Acta Crystallogr., Sect. B*, **B34**, 620 (1978); J. L. Galigné, B. Liautard, S. Peytavin, G. Brun, M. Maurin, J. M. Fabre, E. Torrelles, and L. Giral, *Acta Crystallogr., Sect. B*, **B35**, 1129 (1979); J. L. Galigné, B. Liautard, S. Peytavin, G. Brun, M. Maurin, J. M. Fabre, E. Torrelles, and L. Giral, *Acta Crystallogr., Sect. B*, **B35**, 2609 (1979); J. L. Galigné, S. Peytavin, B. Liautard, and G. Brun, *Cryst. Struct. Commun.*, **9**, 61 (1980).
- 10) G. Brun, S. Peytavin, B. Liautard, M. Maurin, É. Torrelles, J. M. Fabre, and L. Giral, *C. R. Acad. Sci., Ser. C*, **284**, 211 (1977).
- 11) A. Penicaud, P. Batail, K. Bechgaard, and J. Sala-Pala, *Synth. Met.*, **22**, 201 (1988).
- 12) R. E. Dietz, F. R. Merritt, R. Dingle, D. Hone, B. G. Silbernagel, and P. M. Richards, *Phys. Rev. Lett.*, **26**, 1186 (1971); J.-P. Boucher, M. A. Bakheit, M. Nechtschein, M. Villa, G. Bonera, and F. Borsa, *Phys. Rev. B*, **13**, 4098 (1976).
- 13) J. C. Scott, H. J. Pedersen, and K. Bechgaard, *Phys. Rev. Lett.*, **45**, 2125 (1980).
- 14) R. B. Somoano, A. Gupta, V. Hadek, T. Datta, M. Jones, R. Deck, and A. M. Hermann, *J. Chem. Phys.*, **63**, 4970 (1975).
- 15) P. M. Chaikin, R. L. Greene, S. Etemad, and E. Engler, *Phys. Rev. B*, **13**, 1627 (1976).